
JOURNAL OF THE AMERICAN CHEMICAL SOCIETY

DNA-Mediated Acid Catalysis: Calculations of the Rates of DNA-Catalyzed Hydrolyses of Diol Epoxides¹

Gene Lamm, Linda Wong, and George R. Pack*

Contribution from the Department of Biomedical Sciences, University of Illinois College of Medicine, Rockford, Illinois 61107

Received November 6, 1995[⊗]

Abstract: DNA catalyzes the reactions of many small molecules and assists enzymes catalyzing modifications of DNA itself. Previous work by the authors showed that hydronium ions constitute an important component of the counterion atmosphere surrounding polyelectrolytes in general and DNA in particular. It was proposed that local regions at the surface of DNA, termed *acidic domains*, might be responsible for the protonation of epoxides to form reactive intermediates. This acid catalysis is DNA-mediated in the sense that DNA associatively binds the reactant hydronium ions. DNA catalysis of the hydrolysis of the *syn*- and *anti*-7,8-diol 9,10-epoxides of the procarcinogen benzo[*a*]pyrene (*syn*- and *anti*-BPDE) has been investigated for over a decade. Jerina and co-workers have shown that, in the absence of DNA, the observed rate of hydrolysis (k_{obs}) can be represented as the sum of a spontaneous, pH-independent contribution (k_0) and an acid-catalyzed component (k_{H}): $k_{\text{obs}} = k_0 + k_{\text{H}}[\text{H}^+]$, where $[\text{H}^+]$ denotes the (bulk) hydronium ion concentration. An important aspect of that work is that while the acid-catalyzed reactions of both BPDE diastereomers occur via similar mechanisms, considerable differences are found in their rates of hydrolysis. Later work by Jerina involved the catalyzed hydrolysis of *syn*- and *anti*-BPDE by DNA. Typical Michaelis–Menten saturation curves were used to extract apparent rate constants in the presence of DNA. To illustrate the utility of the acidic domains concept in DNA-mediated acid hydrolysis, we have modeled both the intercalative and associative (outside-binding) reaction modes of specific BPDE diastereomers with DNA by combining Poisson–Boltzmann (PB), Monte Carlo, and molecular mechanics techniques. First, the hydronium ion concentration near a B-form model of DNA was obtained by using a previously described PB method for mapping the electrostatic potential in counterion volume elements surrounding DNA. Second, the Metropolis Monte Carlo procedure was used to find the equilibrium distribution of BPDE externally associated with DNA in the PB-calculated electrostatic potential. Finally, the intercalation of a single BPDE molecule into the base-pair stack of DNA was modeled by using AMBER to generate conformations of possible intercalation complexes and then using the PB method to map $[\text{H}^+]$ near the suspected binding sites. Hydrolysis rates for the intercalated molecules were subsequently calculated and combined with external hydrolysis rates to yield total rate curves for the hydrolysis of BPDE as a function of DNA concentration and bulk pH. These curves were then compared with available experimental results. Agreement with experiment was very good in all cases. While use of experimentally derived rate constants practically guarantees reasonable agreement, the calculated hydrolysis rates can be dissected to provide separate intercalated and associated rates and to see how they are individually affected by bulk pH. Furthermore, the application of the acidic domains model to DNA-catalyzed BPDE hydrolysis points out that the measured apparent rate constant for acid-catalyzed hydrolysis can be expressed as the product of the DNA-independent rate constant and the local increase in the hydronium ion concentration over the bulk value.

Introduction

Duplex DNA catalyzes reactions of small molecules such as diol epoxides,^{2–4} nitrogen mustard,⁵ cyclopropylpyrrololindoles,^{6,7} and platinum–triamine complexes.⁸ The cleavage of DNA by the restriction enzymes *ecoRI* and *ecoRV* is a substrate-assisted catalytic process.^{9,10} Other enzyme–DNA reactions involve the protein acting as a general acid or base.¹¹ In these reactions the effective pK_a of the proton donor or acceptor amino acid should be greatly perturbed by the strong electrostatic potential at the DNA surface.¹² We have hypothesized that there is a common mechanism in these and other reactions involving DNA: the electrostatic potential generated by this polyelectrolyte predictably alters the kinetics of proton transfer. In this paper we describe a combination of computational studies designed to test this hypothesis on a system with well-characterized kinetic properties.

The ability of DNA to catalyze the hydrolysis of the diol epoxides of polycyclic aromatic hydrocarbons has been well studied. An example is the 7,8-diol 9,10-epoxide of benzo[*a*]pyrene (BPDE), the metabolic product formed by monooxidation of its parent hydrocarbon. The stereoisomers of the diastereomeric pair in which the 7-hydroxyl is either *syn* or *anti* with respect to the oxirane oxygen have been the subject of the most intense study. Denoted *syn*- and *anti*-BPDE, each of these isomers exists as a pair of enantiomers, the (+) members of which are considered in this study and are depicted in Figure 1. Both *syn*- and *anti*-BPDE have been found to undergo a detoxification reaction resulting in a tetraol that does not react with DNA. Through an alternate mechanism, *anti*-BPDE may instead react with the exocyclic amino group of guanine to form a covalent adduct responsible for carcinogenic mutations. For example, this diastereomer induces a high frequency of G to T transversions in codon 249 of the p53 tumor-suppressor gene, a mutation associated with hepatocellular carcinoma.¹³

Whalen *et al.*¹⁴ showed that kinetic data of BPDE hydrolysis can be accurately fit by

$$k_{\text{obs}} = k_0 + k_{\text{H}}[\text{H}^+] \quad (1)$$

in which k_0 is the rate constant for spontaneous hydrolysis and $k_{\text{H}}[\text{H}^+]$ is the pseudo-first-order rate constant for acid-catalyzed hydrolysis, where $[\text{H}^+]$ is the bulk hydronium ion concentration.

© Abstract published in *Advance ACS Abstracts*, March 15, 1996.

(1) This work was supported in part by Grant No. R01-GM29079 from the NIH.

(2) Islam, N. B.; Whalen, D. L.; Yagi, H.; Jerina, D. M. *J. Am. Chem. Soc.* **1987**, *109*, 2108–2111.

(3) Islam, N. B.; Gupta, S. C.; Yagi, H.; Jerina, D. M.; Whalen, D. L. *J. Am. Chem. Soc.* **1990**, *112*, 6363–6369.

(4) Michaud, D. P.; Gupta, S. C.; Whalen, D. L.; Sayer, J. M.; Jerina, D. M. *Chem. Biol. Interact.* **1983**, *44*, 41–52.

(5) Kohn, K. W.; Hartley, J. A.; Mattes, W. B. *Nucl. Acids Res.* **1987**, *15*, 10531–10549.

(6) Warpehoski, M. A.; Harper, D. E. *J. Am. Chem. Soc.* **1995**, *117*, 2951–2952.

(7) Warpehoski, M. A.; Harper, D. E. *J. Am. Chem. Soc.* **1994**, *116*, 7573–7580.

(8) Anin, M.-F.; Gaucheron, F.; Leng, M. *Nucl. Acids Res.* **1992**, *20*, 4825–4830.

(9) Jeltsch, A.; Alves, J.; Wolfes, H.; Maass, G.; Pingoud, A. *Proc. Natl. Acad. Sci. U.S.A.* **1993**, *90*, 8499–8503.

(10) Jeltsch, A.; Pleckaityte, M.; Selent, U.; Wolfes, H.; Siksny, V.; Pingoud, A. *Gene* **1995**, *157*, 157–162.

(11) Stivers, J. T.; Shuman, S.; Mildvan, A. S. *Biochemistry* **1994**, *33*, 15449–15458.

(12) Lamm, G.; Pack, G. R. *Proc. Natl. Acad. Sci. U.S.A.* **1990**, *87*, 9033–9036.

(13) Bailloul, B.; Brown, K.; Ramsden, N.; Akhurst, R. J.; Fee, F.; Balmain, A. *Environ. Health Perspect.* **1989**, *81*, 23–27.

(14) Whalen, D. L.; Montemarano, J. A.; Thakker, D. R.; Yagi, H.; Jerina, D. M. *J. Am. Chem. Soc.* **1977**, *99*, 5522–5524.

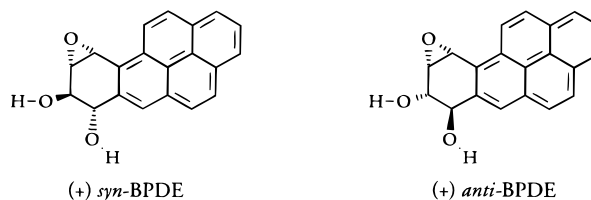


Figure 1. The structures of (+)*syn*- and (+)*anti*-BPDE.

A carbocation intermediate is formed in the spontaneous hydrolysis reaction of *syn*-BPDE. Spontaneous hydrolysis of *anti*-BPDE appears to have a different mechanism, although a carbocationic intermediate is still likely.³ The formation of a carbocation suggests that the diol epoxide can react with nucleophilic sites on DNA as an alkylating agent. Studies of the general acid-catalyzed hydrolysis of *syn*- and *anti*-BPDE point to reactions that involve the formation of a benzylic carbocation intermediate in the rate-determining step. In the reactions of both diastereomers, H_3O^+ can act as a general-acid catalyst in a mechanism in which the rate-determining step is proton transfer to the epoxide oxygen in concert with a benzylic C–O bond cleavage.³

In 1980, Slaga and co-workers¹⁵ showed that the rate of hydrolysis of *anti*-BPDE increases significantly in the presence of DNA. Michaud *et al.*⁴ measured the pH dependence of this reaction and suggested that hydrolysis in the presence of DNA is acid catalyzed. It is generally accepted that the formation of noncovalent BPDE–DNA complexes precedes covalent adduct formation.^{16,17} These noncovalent complexes have been categorized as either “Site I” or “Site II”.¹⁸ Site I complexes involve intercalation into the base-pair stack of DNA and thus require that the conformation of the nucleic acid change. Site II complexes involve little or no stacking of the planar portion of BPDE with the nucleotide bases and so are regarded as external site formations. It has been suggested that an intercalation complex would precede hydrolysis.¹⁹ Studies of the pH dependence of DNA-catalyzed hydrolysis of *syn*- and *anti*-BPDE show that an intercalation complex is not an absolute requirement for catalysis since the reaction is also catalyzed by single-stranded poly(dG) and poly(dA).² In fact, poly(dG) is a more efficient catalyst than double-stranded DNA.

The increase in the hydrolysis rate with increasing DNA concentration (at constant pH) suggests that general acid catalysis would occur with DNA being the proton donor. While MacLeod and Zachary²⁰ have suggested that the donor proton may be covalently attached to the exocyclic amino group of guanine, this need not be the case. The proton donor may reside within the minor groove of the nucleic acid as part of a local *acidic domain*.¹² This hydronium ion, as a constituent of the ionic atmosphere of DNA, is bound to the polyelectrolyte molecule in the same sense that condensed counterions are bound. The transient nature of the H_3O^+ species suggests an alternate way of viewing the acidic domains at the DNA surface, namely, as regions in which the effective pK_a of local water

(15) Koostra, A.; Haas, B. L.; Slaga, T. J. *Biochem. Biophys. Res. Commun.* **1980**, *94*, 1432–1438.

(16) Meehan, T.; Gamper, H.; Becker, J. F. *J. Biol. Chem.* **1982**, *257*, 10479–10485.

(17) Geacintov, N. E. In *Polycyclic Aromatic Hydrocarbon Carcinogenesis: Structure Activity Relationships*; Yang, S. K., Silverman, B. D., Eds.; CRC Press: Boca Raton, 1988; Vol. 1, pp 181–206.

(18) Geacintov, N. E.; Cosman, M.; Mao, B.; Alfano, A.; Ibanez, V.; Harvey, R. *Carcinogenesis* **1991**, *12*, 2099–2108.

(19) MacLeod, M. C. *J. Theor. Biol.* **1990**, *142*, 113–122.

(20) MacLeod, M. C.; Zachary, K. L. *Carcinogenesis* **1985**, *6*, 147–149.

molecules is increased by the large negative electrostatic potential generated by the phosphate groups of DNA.

Theory

In the absence of DNA, BPDE hydrolysis is described by eq 1 with $[H^+]$ constant and determined by the pH of the solution. DNA-catalyzed hydrolysis contains contributions from three reaction mechanisms: Site I intercalated complexes, Site II externally associated complexes, and DNA-independent (free) hydrolysis. Site II and free hydrolysis can be unified if we modify eq 1 to allow $[H^+]$ to vary throughout the volume V of the system:

$$k_{II} = V^{-1} \int (k_0 + k_H[H^+]) dV \quad (2)$$

This result can be further generalized to account for a non-uniform distribution of BPDE:

$$k_{II} = \frac{\int (k_0 + k_H[H^+]) [BPDE] dV}{\int [BPDE] dV} \quad (3)$$

In writing eq 3 we have assumed that the spontaneous rate constant k_0 and the acid-catalyzed rate constant k_H are constant throughout V and retain their values measured in the absence of DNA. This assumption is reasonable for externally associated, noncovalently bound BPDE.

Site I-mediated hydrolysis may also be described by a generalization of eq 1:

$$k_I = \sum_j w_j (k'_0 + k'_H[H^+]_j) \quad (4)$$

where we sum over all intercalation binding sites j , each having a probable weight w_j . We have used a "prime" notation to indicate that intercalation may lead to spontaneous and acid-catalyzed rate constants with different values than those in the bulk solution.

Equations 3 and 4 may be combined in a simple two-state model to give the total rate of hydrolysis if the relative fraction θ of intercalated BPDE is known:

$$k_{\text{calc}} = \theta k_I + (1 - \theta) k_{II} \quad (5)$$

where θ depends on the DNA concentration. We describe below how various computational techniques were applied in the calculation of rate curves based on eq 5 for DNA-catalyzed hydrolysis of BPDE. Results are presented for both the *syn*- and *anti*-diastereomers of BPDE as a function of DNA concentration and bulk pH. Comparison with experiment allowed the validity of the assumptions used in developing eq 5 to be tested.

Methods

Evaluation of eq 5 for a specific diastereomer at a given DNA concentration and bulk pH entailed the following steps:

- (1) Define the system including the discretization of space into finite volumes.
- (2) Calculate the $[H^+]$ distribution throughout the system volume.
- (3) Calculate the [BPDE] distribution throughout the system volume.
- (4) Calculate the fraction θ of BPDE that is intercalated.
- (5) Determine the intercalation sites for BPDE in a base-pair stack of DNA and $[H^+]$ at these sites.
- (6) Obtain values for the spontaneous (k_0 , k'_0) and acid-catalyzed (k_H , k'_H) hydrolysis rate constants.

Definition of the System. The system used for the Site II calculations consisted of an all-atom model of B-form poly(dG)•poly(dC) and BPDE in a dielectric continuum. Previous

Poisson–Boltzmann calculations²¹ have shown that, for canonical B-DNA, the electrostatic potential in the environment is largely independent of nucleotide sequence. The helical axis of DNA was chosen to be coincident with the axis of the cylindrical system cell of height 33.8 Å and radius 170 Å resulting in a DNA concentration of 10.8 mM. Other concentrations of DNA are obtained by adjusting this system radius. A series of cross sections, 1.69 Å in height and perpendicular to the helical axis, was defined and a rolling-sphere algorithm used to generate a curvilinear lattice contoured to the static DNA surface. The fixed atomic charges of DNA were distributed among interior parallelepiped cells according to each cell's three-dimensional overlap with the atomic van der Waals spheres. Cells within the DNA boundary were assigned a dielectric constant of 2 while those of the environment were set to 78.4; the former approximates the high-frequency (electronic) dielectric coefficient of hydrocarbons while the latter represents the dielectric constant of bulk water. A value of 2 has been used for Poisson–Boltzmann calculations of proteins²² although higher values have also been suggested.²³ Cell volumes and shared surface areas among neighboring cells were recorded to be used in the following Poisson–Boltzmann algorithm.

Calculation of $[H^+]$. The distribution of hydrogen ions in a dielectric continuum representing an electrolyte solution around DNA was obtained by solving the nonlinear Poisson–Boltzmann equation on a curvilinear 3-dimensional lattice contoured to the DNA surface.²⁴ Briefly, the Poisson equation for the electrostatic potential was combined with the nonlinear Boltzmann equation for the distribution of (univalent) counterions. The finite difference version of the Poisson equation for the electrostatic potential ϕ_i at cell location i on a curvilinear grid is

$$\phi_i = \frac{[4\pi v_i \rho_i / \epsilon_i + \sum_j (\phi_j \epsilon_{ij} S_{ij} / r_{ij})]}{\sum_j (\epsilon_{ij} S_{ij} / r_{ij})} \quad (6)$$

where v_i is the volume of cell i , ρ_i is the total charge density, $\epsilon_{ij} = (\epsilon_i + \epsilon_j)/2$ is the arithmetic average of the dielectric constants in cells i and j , S_{ij} is the shared surface area of these cells, and r_{ij} is the distance between cell centers. Summations are taken over all cells j sharing a surface with a given cell i . Inside the DNA the charge within each cell was fixed as calculated from the overlap with the atomic van der Waals spheres and provided a charge density $\rho_i = q_i/v_i$. The total charge density in each cell in the environment was obtained from the individual ionic charge densities by summation: $\rho_i = \sum_k \rho_i^k$. The Boltzmann equation for each ion type was then written

$$\rho_i^k = \frac{N_k \exp(-\beta z_k \phi_i)}{\sum_i v_i \exp(-\beta z_k \phi_i)} \quad (7)$$

in which z_k is the ion valence and N_k is the total number of ions

(21) Pack, G. R.; Wong, L.; Prasad, C. V. *Nucl. Acids Res.* **1986**, *14*, 1479–1493.

(22) Klapper, I.; Hagstrom, R.; Fine, R.; Sharp, K.; Honig, B. *Proteins: Structure, Function and Genetics* **1986**, *1*, 47–59.

(23) Mohan, V.; Davis, M. E.; McCammon, J. A.; Pettitt, B. M. *J. Phys. Chem.* **1992**, *96*, 6428–6431.

(24) Pack, G. R.; Garrett, G. A.; Wong, L.; Lamm, G. *Biophys. J.* **1993**, *65*, 1363–1370.

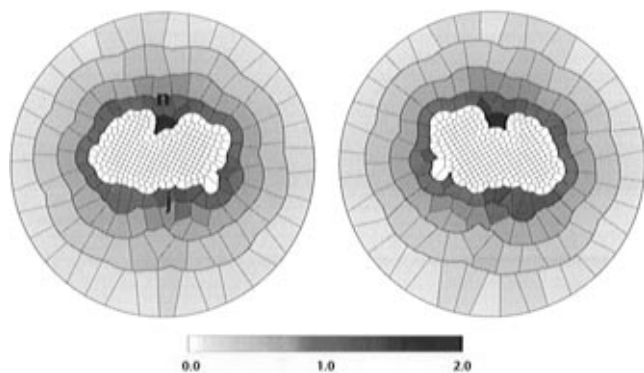


Figure 2. Cross-sectional views, 1.69 Å apart, perpendicular to the helical axis of B-DNA showing the division of space into a curvilinear grid of finite volume elements. The value of $\Delta(\text{p[H]})$ in each of the finite elements in the environment surrounding DNA is shown in gray scale. The unshaded central portion is occupied by DNA. The approximate regions of the major and minor grooves are indicated by a “j” and an “n”, respectively.

of type k within the system. One species was the hydronium ion, represented as H^+ . Using the definition

$$\text{p[H]}_i = -\log[\text{H}^+]_i = \text{pH} + 2.303^{-1}\beta\phi_i \quad (8)$$

the local hydrogen ion concentration could be described in terms of the bulk solution pH and the local electrostatic potential.

The PB solution to eqs 6 and 7 is insensitive to the bulk pH since hydronium ions are several orders of magnitude less numerous than the accompanying counterions. Thus, once the PB equation had been solved and the spatial distribution of hydronium ions, $[\text{H}^+]_i^{\text{ref}}$, had been obtained for a given DNA concentration and reference bulk pH, hydronium ion concentrations at other bulk pH values were readily obtained from the approximate invariant $\Delta(\text{p[H]}_i)$:

$$\text{p[H]}_i - \text{pH} = \Delta(\text{p[H]}_i) = \text{p[H]}_i^{\text{ref}} - \text{pH}^{\text{ref}} \quad (9)$$

Figure 2 presents cross-sectional maps of $\Delta(\text{p[H]}_i)$ for two planes, 1.69 Å apart, for B-form poly(dG)·poly(dC) at 298 K.

Calculation of [BPDE]. As discussed above, noncovalent binding of benzo[*a*]pyrene diol epoxide to DNA was assumed to involve a multiplicity of sites categorizable as either Site I (intercalation) or Site II (external association). The equilibrium distribution of BPDE can be determined by sampling Metropolis Monte Carlo energy configurations of BPDE in the electrostatic field of DNA. A BPDE molecule was randomly translated and rotated within a periodic box that extended radially to the cylinder walls and axially for 10 nucleotide pairs (33.8 Å) of a rigid B-DNA helical duplex. The grid of finite volume elements previously defined for the Poisson–Boltzmann calculation was used to generate histograms that report the probability density for individual atoms of BPDE residing in each spatial location.

The nonelectrostatic potential energy of the system was calculated as the sum of all pairwise inverse 6–12 interactions of BPDE with DNA. Parameters for the 6–12 interactions were taken from the AMBER parameter set.²⁵ To calculate the electrostatic energy in a way that included the electrostatic contribution from the full, electrically neutral system, determination of the potential in the volume element in which each atom resides was necessary. The electrostatic contribution to the energy of the i th atom in the k th volume element was defined as the product of the electrostatic potential in cell k and the

charge of atom i . The full energy expression could then be written

$$U = \sum_i^{\text{BPDE}} \left[\sum_k (\phi_k q_i) + \sum_m^{\text{DNA}} (a_i a_m / r_{im}^{12} - c_i c_m / r_{im}^6) \right] \quad (10)$$

where ϕ_k was the full (DNA plus counterions) PB electrostatic potential in the k th volume element, the element in which atom i of the diol epoxide was located. By calculating the electrostatic potential energy as the interaction of the diol epoxide atomic charges with the average electrostatic potential of the DNA–electrolyte system, average properties of the BPDE–DNA system could be obtained. Further discussions of this method, including a discussion of the convergence properties, are given elsewhere.²⁶

Analysis of the spatial distribution of an asymmetric polyatomic molecule is more complicated than that required for simple counterions. The mechanism of acid-catalyzed carbocation formation requires that a proton be transferred to the oxirane oxygen making the location of this atom paramount. A histogram for this oxygen was maintained during the calculation by recording the number of configurations in which this atom occurred in each volume element. The fraction of configurations in which a given volume element contained the oxirane oxygen was converted to probability densities (having the dimensions of concentration) at the completion of the calculation and is denoted by [BPDE].

This procedure also allowed the determination of bound vs free BPDE by obtaining the average energy for a BPDE molecule whose oxirane oxygen resided in a particular volume element. We have shown²⁷ that a consistent and reliable criterion for a counterion to be bound in the sense of counterion-condensation theory is that its electrostatic energy is less than $-kT$. Using this criterion, we could then calculate the individual contributions of Site II and free hydrolysis to the total rate for DNA-catalyzed BPDE hydrolysis.

Calculation of θ , the Fraction of BPDE Intercalated. Michaud *et al.*⁴ and Islam *et al.*² have measured equilibrium constants for *anti*- and *syn*-BPDE–DNA binding, based on a similar two-state model. Denoting the concentration of Site I-bound, Site II-bound, and free BPDE by $[\text{B}_I]$, $[\text{B}_{II}]$, and $[\text{F}]$, the measured equilibrium binding constant is given by

$$K_{\text{eq}} = \frac{[\text{B}_I]}{([\text{B}_{II}] + [\text{F}])[\text{DNA}]} \quad (11)$$

The fraction of BPDE that is intercalated can be written as

$$\theta = [\text{B}_I]/([\text{B}_I] + [\text{B}_{II}] + [\text{F}]) \quad (12)$$

or, similarly,

$$\theta = \frac{K_{\text{eq}}}{K_{\text{eq}} + 1/[\text{DNA}]} \quad (13)$$

which is equivalent to that used by Michaud and by Islam. The reported equilibrium constants lead to

$$\theta_{\text{syn}} = 1070M^{-1}/(1070M^{-1} + 1/[\text{DNA}])$$

and

(26) Pack, G. R.; Lamm, G.; Wong, L. *Int. J. Quantum Chem.* **1995**, *QBS22*, 29–37.

(27) Lamm, G.; Wong, L.; Pack, G. R. *Biopolymers* **1994**, *34*, 227–237.

(25) Weiner, S. J.; Kollman, P. A.; Nguyen, D. T.; Case, D. A. *J. Comp. Chem.* **1986**, *7*, 230–252.

$$\theta_{\text{anti}} = 2400M^{-1}/(2400M^{-1} + 1/[\text{DNA}]) \quad (14)$$

Determination of the Intercalation Sites and Their [H⁺] Values. Numerous conformations are possible for the noncovalent intercalated complex. By analogy with the known structures of covalently bound diol epoxides, it can be inferred that physically bound BPDE may be oriented in the minor groove with its planar portion approximately parallel to the DNA-helix axis or it may intercalate with its plane perpendicular to the helical axis. This analogy should not be overextended. Covalent adducts are formed by attachment of the benzylic carbon of the oxirane moiety with the deoxyguanosine exocyclic NH₂ residing in the minor groove. However, this does not necessarily imply that an intercalation complex preceding hydroxylation would have the oxirane ring oriented toward the minor groove. An exhaustive search of possible structures and subsequent Boltzmann averaging of their contributions to the hydrolysis rates was not feasible. Nonetheless, it is possible to generate representative structures and determine whether their characteristics are compatible with experimental data.

Generation of representative structures for intercalation complexes is described in detail elsewhere.²⁸ Solution conformations of the covalent adduct of (+)-*anti*-BPDE with the exocyclic amino group of G₆ of this oligonucleotide duplex are known, having been learned from NMR measurements and energy minimization.^{29–31} Reasonable results for BPDE–DNA intercalation complexes were obtained using AMBER²⁸ molecular mechanics calculations with TIP3P waters³² as implemented in HyperChem.³³ Model conformations were constructed from the 11-mer d(CCATC₅G₆C₇TACC)–d(GGTAG₁₆C₁₇G₁₈ATGG) with two intercalation sites: in the first, the BPDE molecule was placed between the C₅G₁₈ and G₆C₁₇ base pairs; in the second, a site between the G₆C₁₇ and C₇G₁₇ base pairs was chosen. This provided major and minor groove locations for the epoxide moiety with both C(3′-5′)G and G(3′-5′)C sites in a sequence to which BPDE is known to bind.^{29–31} Two orientations for BPDE in each intercalation site were constructed, one with the oxirane group in the major groove and the other with the oxirane oriented toward the minor groove, providing four possible intercalation complexes for each diastereomer. A periodic box, 5 Å larger in each dimension than the minimum box enclosing the complex, was filled with TIP3P waters to simulate two hydration shells. Twenty-two sodium counterions were added to neutralize the system. Unconstrained energy minimizations using periodic boundary conditions with the minimum image restriction resulted in four representative intercalation geometries for each BPDE diastereomer.

Poisson–Boltzmann potentials were calculated in a grid of volume elements generated around each optimized intercalated structure in a manner similar to that described previously and the positions of the oxirane oxygen were recorded relative to

(28) Pack, G. R.; Wong, L. *Chem. Phys.* In press.

(29) Cosman, M.; De Los Santos, C.; Fiala, R.; Hingerty, B. E.; Singh, S. B.; Ibanez, V.; Margulis, L. A.; Live, D.; Geacintov, N. E.; Broyde, S.; Patel, D. J. *Proc. Natl. Acad. Sci. U.S.A.* **1992**, *89*, 1914–1918.

(30) Cosman, M.; De Los Santos, C.; Fiala, R.; Hingerty, B. E.; Ibanez, V.; Luna, E.; Harvey, R. G.; Geacintov, N. E.; Broyde, S.; Patel, D. J. *Biochemistry* **1993**, *32*, 4145–4155.

(31) Cosman, M.; Fiala, R.; Hingerty, B. E.; Amin, S.; Geacintov, N. E.; Broyde, S.; Patel, D. J. *Biochemistry* **1994**, *33*, 11518–11527.

(32) Jorgenson, W. L.; Chandrasekhar, J.; Madura, J. D.; Impey, R. W.; Klein, M. L. *J. Chem. Phys.* **1983**, *79*, 926–935.

(33) *HyperChem for Windows: Release 4*; Hypercube, Inc.: Waterloo, Ontario, Canada, 1994.

(34) Eigen, M. *Angew. Chem., Int. Ed. Engl.* **1964**, *3*, 1–72.

(35) Eigen, M.; De Maeyer, L. *Proc. R. Soc. London, A* **1958**, *247*, 505–533.

this grid. For *syn*-BPDE, the values of p[H]_I (in a reference system at bulk pH 7) for the cell in which the epoxide oxygen resides for the four *syn*-BPDE–DNA intercalation complexes were 4.5, 4.9, 5.6, and 4.4. The corresponding p[H]_I values for the environmental cell closest to the oxygen were 5.5, 5.8, 6.2, and 5.8. For *anti*-BPDE–DNA intercalation complexes, the values of p[H]_I for the cell in which the oxygen resides for the four calculated intercalation structures were 4.2, 3.4, 4.3, and 4.3 and those of the closest environmental cell were 5.5, 5.2, 5.5, and 5.8. Assigning equal weights to all intercalation complexes for a given diastereomer (*i.e.*, $w_j = 1$) and choosing a p[H] value for Site I as the average among the eight p[H]_I values gives

$$p[\text{H}]_I^{\text{syn}} = 5.3 \pm 0.7 \quad \text{and} \quad p[\text{H}]_I^{\text{anti}} = 4.8 \pm 0.8 \quad (15)$$

Determination of the Spontaneous and Acid-Catalyzed Hydrolysis Rates k_0 and k_H . Whalen *et al.*¹⁴ measured the spontaneous and acid-catalyzed hydrolysis in the absence of DNA for both diastereomers investigated here. They found the first- and second-order rate constants

$$k_0^{\text{syn}} = 1.8 \times 10^{-2} \text{ s}^{-1} \quad \text{and} \quad k_0^{\text{anti}} = 3.0 \times 10^{-4} \text{ s}^{-1} \quad (16a)$$

$$k_H^{\text{syn}} = 550 \text{ M}^{-1} \text{ s}^{-1} \quad \text{and} \quad k_H^{\text{anti}} = 1400 \text{ M}^{-1} \text{ s}^{-1} \quad (16b)$$

We use these values for free and Site II (externally associated) interactions.

For Site I complexes, changes in the conformation or electronic structure of BPDE induced by intercalation and/or disruption of water structure at the surface of DNA could lead to changes in any of the above hydrolysis rate constants. Michaud *et al.*⁴ and Islam *et al.*² have fit data for DNA-catalyzed *anti*- and *syn*-BPDE hydrolysis and obtained apparent first- and second-order rate constants for Site I complexes. It is reasonable to assume that intercalation alters the structure of BPDE sufficiently to change the first-order hydrolysis rate constant. Comparison of the intercalation structures generated above with the native forms of *syn*- and *anti*-BPDE shows considerable distortion. While this would be expected to affect hydrolysis rates, quantitative predictions would require detailed quantum mechanical calculations. The Michaud–Islam first-order values of k_0 for intercalated BPDE are

$$k_0^{\text{syn}} = 3.3 \times 10^{-2} \text{ s}^{-1} \quad \text{and} \quad k_0^{\text{anti}} = 1.4 \times 10^{-3} \text{ s}^{-1} \quad (17)$$

(Michaud and Islam use the subscript “cat” to designate rate constants of the intercalated molecules; we use the “prime” notation for the same quantity.)

Michaud *et al.*⁴ and Islam *et al.*² also determined second-order rate constants for physically bound BPDE. However, their analyses ignored changes in the local hydrogen ion concentration at the binding site due to the electrostatic field of DNA. This results in an effective second-order rate constant given by

$$k_H^{\text{eff}} = k_H[\text{H}^+]_I/[\text{H}^+]_{\text{bulk}} = k_H 10^{\Delta(\text{p[H]})} \quad (18)$$

where $\Delta(\text{p[H]}) = \text{pH} - \text{p[H]}_I$. This change in the second-order rate constant was interpreted as binding-induced by Michaud and by Islam. In fact, the experimentally determined rate constants given by Michaud and by Islam can be used to provide p[H]_I at the intercalation site(s) (for reference pH 7):

$$\text{syn:} \quad \text{p[H]}_I = 7 - \log(30600/550) = 5.25$$

$$\text{anti: } p[H]_I = 7 - \log(85500/1400) = 5.21 \quad (19)$$

The closeness of these site $p[H]_I$ values and their agreement with the estimated values given in eq 15 demonstrate both the validity and utility of the acidic domains concept. Thus, *the apparent change in the second-order rate for the DNA-catalyzed hydrolysis of BPDE with respect to free hydrolysis actually results from a change in the local concentration of hydrogen ions.* Therefore, in the evaluation of eq 20 we used the free-hydrolysis values of eq 16b for the Site I second-order rate constants.

Results

Having calculated the components of the rate constants, k_I , k_{II} , and k_{calc} (eqs 3, 4, and 5), the overall rate curves for DNA-mediated acid hydrolysis were evaluated for different concentrations of DNA as a function of bulk pH. As mentioned earlier, the Poisson–Boltzmann calculation of electrostatic potentials, and hence the $[H^+]$ concentrations, needed to be done only once at a reference bulk pH. Additional $[H^+]$ values for other bulk pH choices were readily obtained through eq 9. Writing $\Delta pH = pH - pH^{\text{ref}}$ as the difference between the reference bulk pH (7.0) and the bulk pH for which the rate curve was calculated, we combined eqs 3, 4, and 5 with the assumptions discussed above to obtain

$$k_{\text{calc}} = \frac{\theta(k'_0 + k_H[H^+]_I 10^{-\Delta pH}) + \sum_i (k_0 + k_H[H^+]_I 10^{-\Delta pH}) [BPDE]_i \nu_i}{(1 - \theta) \sum_i [BPDE]_i \nu_i} \quad (20)$$

where integrals have been converted to summations over all volume elements.

Islam *et al.*² obtained experimental DNA-catalyzed *syn*-BPDE hydrolysis rates for DNA concentrations varying from 0 to 1.2 mM and for pH values of 5.7, 6.07, and 7.0. These observed rates are compared with the results obtained using eq 20 with the parameters of eqs 14, 16, 17, and 19 in Figure 3. The slight deviation between the experimental values and the calculated curves, particularly at lower pH, results from using the experimentally determined rate constants. Use of eq 20 to fit the experimental curves would yield slightly different rate constants but a more accurate fit.

Michaud *et al.*³ obtained experimental DNA-catalyzed *anti*-BPDE hydrolysis rates for DNA concentrations varying from 0 to 3.0 mM and for bulk pH values of 6.5, 7.0, and 7.5. These values are compared with the results obtained using eq 20 in Figure 4 and agreement is close, as expected.

Use of experimentally determined rate constants k_0 , k'_0 , and k_H in eq 20 guarantees that the calculated hydrolysis rate curves will not deviate greatly from the experimental values. Equation 20 is derived, however, from a physical model of the experiments and can be used to extract the separate contributions from Site I, Site II, and free hydrolysis. Figure 5 shows these contributions for *syn*-BPDE at a bulk pH of 5.7. Intercalated Site I dominates the hydrolysis rate for most of the DNA concentration range due to the relatively high concentration of hydronium ions near the epoxide oxygen of the intercalated BPDE ($p[H]_I = 5.25$). Also, only for DNA concentrations larger than about 0.9 mM does the Site II contribution become larger than that for free hydrolysis. The total rate of hydrolysis for all nonintercalated BPDE—the sum of the Site II and free rates—is also plotted for comparison.

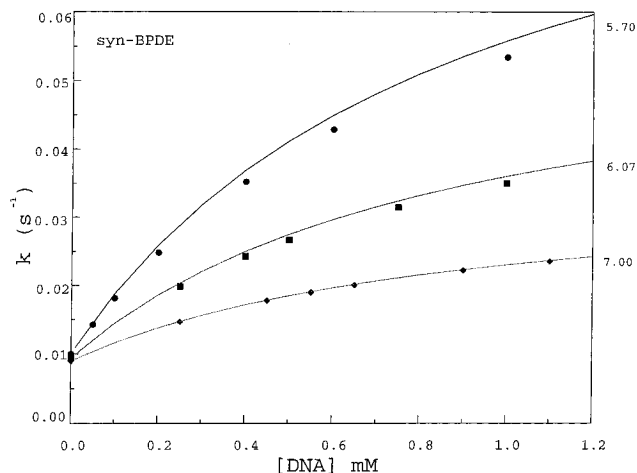


Figure 3. A comparison of the experimentally-observed rates (symbols, replotted from Islam *et al.*, 1987) and calculated rate curves (smooth curves) for *syn*-BPDE for the experimental bulk pH values as a function of DNA concentration.

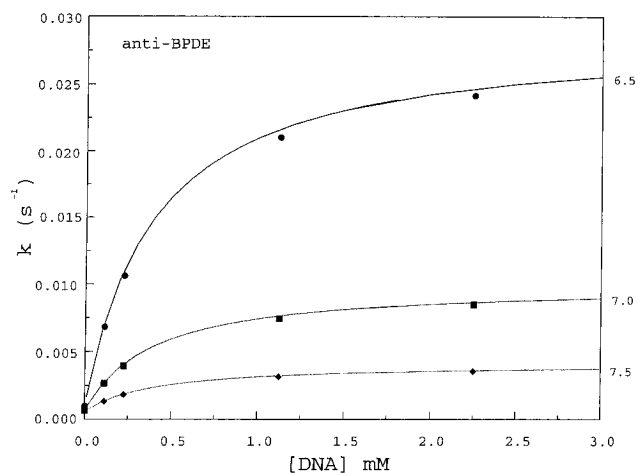


Figure 4. A comparison of the experimentally-observed rates (symbols, replotted from Michaud *et al.*, 1983) and calculated rate curves (smooth curves) for *anti*-BPDE for the experimental bulk pH values as a function of DNA concentration.

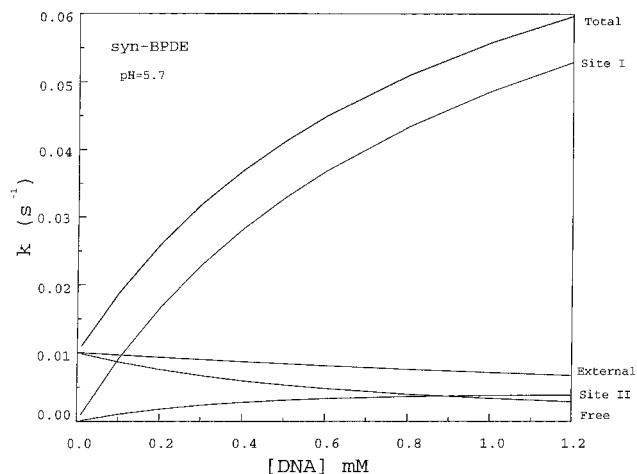


Figure 5. Calculated hydrolysis rate curves for *syn*-BPDE showing the Site I, Site II, free, and external (Site II + free) contributions to the total rate as a function of DNA concentration for a bulk pH value of 5.7.

The major contribution to DNA-mediated BPDE hydrolysis results from intercalation. Figure 6 shows the change in intercalated BPDE hydrolysis as a function of the local hydronium concentration for a narrow range of $p[H]_I$ values.

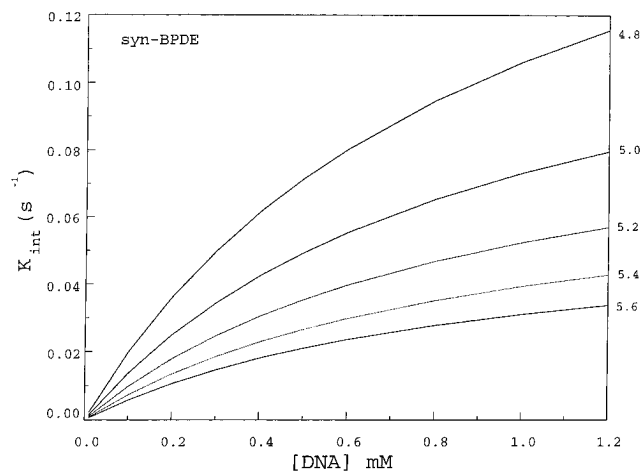


Figure 6. The intercalation contribution to the hydrolysis rate for *syn*-BPDE as a function of DNA concentration for several p[H] values at the intercalation site.

Fitting experimental data to eq 20 thus allows the local (average) hydronium ion concentration to be determined quite accurately.

One aspect of the experiments we have not discussed is the effect of ionic strength on the hydrolysis rate. The influence of ionic strength on electrostatic potentials and counterion concentrations near DNA has been discussed in previous work.²⁷ Knowledge of the relative change in the local electrostatic potential as the bulk ionic strength is altered readily provides the change in the local hydronium ion concentration (via eq 8) and therefore the intercalated hydrolysis rate constant (via the first term in eq 20). A difficulty arises because the hydrolysis rate depends on the local hydrogen ion concentration and also on the association constant: both quantities are affected by the ionic strength. The present approach to the prediction of overall hydrolysis rates would require the association rate constant as a function of ionic strength to predict the salt-dependence of the hydrolysis rate.

Conclusions

The model on which the present investigation is based gives some insight into the mechanism of a specific catalytic function of DNA: the DNA-mediated acid hydrolysis of benzo[*a*]pyrene diol epoxide. The calculations show that a minor, yet significant, fraction of hydrolysis results from the external association of BPDE with DNA. The hydrolysis rate constants for Site II associative binding are well represented by those experimentally obtained in the absence of DNA. The major contribution to catalyzed hydrolysis occurs via intercalation of a BPDE molecule into the base pair stack of DNA. The increase in the spontaneous hydrolysis rate constant of the intercalated molecule relative to that measured in the absence of DNA is attributed to environmental effects and/or conformational change in the intercalated molecule. In contrast, the acid-catalyzed rate

constant for BPDE retains its DNA-free value even when intercalated. The local increase in the hydronium ion concentration over its bulk value results in a change in the "apparent" acid-catalyzed rate constant which can be calculated using standard Poisson–Boltzmann theory. The acidic domains concept thus provides a natural framework for analyzing the DNA-induced rate enhancement for the hydrolysis of *syn*- and *anti*-BPDE.

It should be emphasized that the location of the proton immediately prior to transfer to the epoxide oxygen is not addressed in these calculations. The large negative electrostatic potential at the DNA surface increases the apparent pK_a of each species in this domain. The H_3O^+ species is stabilized in this region and the quantitative expression of this is given by local p[H] values. Michaud *et al.*⁴ and Islam *et al.*² have suggested that the proton donor could be a protonated phosphodiester group or nucleic acid base. MacLeod and Zachary²⁰ have argued for the involvement of the exocyclic amino group of deoxyguanosine as a general acid. The extremely high mobility of protons leads to a mean lifetime of approximately 10^{-12} s for an H_3O^+ ion with a mean interval between the associations of a given water molecule with a proton of approximately 5×10^{-4} s in pure water at 25 °C.^{32,33} The rates of proton transfer undoubtedly are altered at the DNA surface but the protons of the acidic domains are expected to retain a very high mobility. It is our approach to view the donors as transiently protonated surface water molecules, recognizing that $\Delta(p[H]_i)$ calculated in this manner is an approximation to the increase in the apparent pK_a of the proton acceptor, the diol epoxide.

The present calculations indicate that in at least one well-characterized system, the primary catalytic effect of DNA is to increase the rate constant for acid catalysis in a way that is predictable from the electrostatic potential. This is accomplished by stabilizing the cationic intermediate in the reaction in the strongly negative DNA-induced electrostatic potential. This electrostatic stabilization must also affect the pK_a s of ionizable residues of enzymes such as EcoRI DNA methyltransferase whose activity is dependent on the presence of these residues.³⁶ The magnitude of the pK_a shift induced by binding to DNA is dependent on the location of these groups in the enzyme–DNA complex. Based on the calculations discussed above, those groups in the grooves, particularly in the minor groove, would experience the largest shift. Use of computed electrostatic potential maps for protein–DNA complexes should provide additional insight into general and specific acid–base catalytic mechanisms. We expect the acidic domains concept of counterion condensation theory to be useful in interpreting other DNA-mediated catalytic reactions of small or site-specific molecules and that much of DNA catalysis can be understood in terms of DNA-mediated acid catalysis.

JA953724X

(36) Mashoon, N.; Reich, N. O. *Biochemistry* **1994**, *33*, 7113–7119.